Polymer Nanocomposites for Wind Energy Applications: Perspectives and Computational Modeling

L. Mishnaevsky Jr.[1], H.W. Zhou[2], R.D. Peng[2], G. Dai[1], H.W. Wang[3]

[1] *Technical University of Denmark, Department of Wind Energy, Risø Campus,*
Frederiksborgvej 399, DK-4000 Roskilde, Denmark
[2] *China University of Mining and Technology, 100083 Beijing, China*
[3] *School of Mechanical Engineering, Tianjin University of Commerce, 300134 Tianjin, China*

Strength and reliability of wind blades produced from polymer composites are the important preconditions for the successful development of wind energy. One of the ways to increase the reliability and lifetime of polymer matrix composites is the nanoengineering of matrix or fiber / matrix interfaces in these composites. The potential and results of nanoclay reinforcements for the improvement of the mechanical properties of polymer composites are investigated using continuum mechanics and micromechanics methods and effective phase model. It is demonstrated that nanoreinforcement allows increasing the stiffness and strength of composites.

1. INTRODUCTION

Perspectives of development of wind energy depend on the reliability of wind turbine parts, in particular, wind blades. The wind blades, produced from polymer composites, should serve for 20-25 years, with minimum maintenance and repair [1]. One of the ways to increase the reliability and lifetime of polymer matrix composites is the nanoengineering of matrix or fiber/matrix interfaces in these composites. Adding small amount of nanoparticles reinforcement can lead to the qualitative improvement of the strength and stiffness of polymers.

In a number of investigations, drastic improvements of mechanical properties and toughness of materials due to small additions of nanoparticles have been observed, for instance, 10 to 50 % higher static tensile strength and modulus and 74 % higher fatigue lifetime in hybrid CFRP (carbon fiber reinforced plastic) with 3 % wt of NC (nanoclay) [2], 34 % higher Young's modulus and 25 % higher tensile strength in nanoclay / epoxy composite with 5 wt % of NC [3], 30 % higher UTS and 38 % or higher Young's modulus, 10.5 % flexural strength and 25 % flexural modulus , 70 % ILSS and 25 % microhardness for 5 % NC in epoxy / glass fibers/nanoclay hybrid composites (HC) [4], 175 % higher yield stress, and 200 % tensile modulus in nylon with 5 wt % clay [5, 6], etc. While the nanoparticle reinforced materials have been rather expensive a few years ago, now their prices tend to reduce, and their broad use can be expected in near future. So, the question arises: can one use nanoreinforcement and nanoengineering as sources of the increasing of damage and fatigue resistance of composites for wind energy applications?

In this paper, we seek to carry out computational micromechanical analysis of the effect of structures of nanocomposites on their mechanical and strength properties. 3D micromechanical FE models of nanocomposites were developed and used to predict the elastic and strength properties of the materials and the effect of the

nano-reinforcement on the properties. The results of the investigation are expected to provide some design parameters for the microstructural optimization of the nanocomposites.

2. COMPUTATIONAL MODELLING OF NANOREINFORCED COMPOSITES

2.1 Computational Tools and Programs

The 3D micromechanical models of a polymer reinforced by nanoclay particles of different shapes were generated with the use of the program code "Nanocomp3D" written in ABAQUS Python Development Environment. The unit cells included nanoparticles of different shapes and orientations, surrounded by multilayered effective interfaces. The term "effective interface" means here the interface / interphase layer between the matrix and a particle, reflecting the modified structure of polymer near the nanoparticles.

The generalized effective interface model (GEIM), developed by Wang et al. [10] considers the effective interface which consists of several (e.g., two) sublayers, with different properties, typically the stronger layers are outer layers. The effective interface layers (or some of their sublayers) are allowed to overlap, thus, reflecting the fact that the peculiar properties of these regions are caused by modified local atomistic structures, molecular structures or diffusion processes, and do not represent separate phases.

The overlapping of effective interfaces or sublayers of the effective interfaces was realized using Boolean operations in ABAQUS. Fig. 1 shows several examples of the 3D unit cells of nanoclay reinforced epoxy considered in our simulations. The mechanical properties of the phases are given in [10].

2.2 Effect of Nanoreinforcement on Elastic Properties

In order to analyze the effect of nanoreinforcement

on the elastic prpeties of composite, we carried out a series of numerical experiments. A number of unit cells with various distribution of nanoclay were generated, and tested in the models. A series of computational simulations has been carried out, using the developed numerical tools. The simulations were carried out using the commercial finite element software ABAQUS. Tensile stress strain curves and stress-damage curves for the different shapes and arrangements of the nanoparticles were determined.
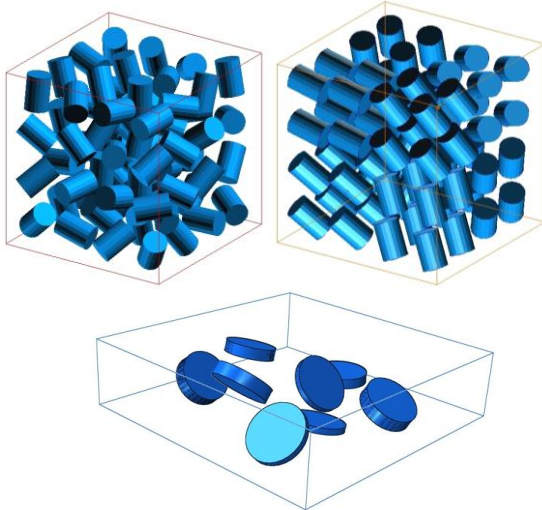

Fig. 1 – Examples of multiparticle unit cells with various distribution of nanoparticles. Idealy random and correlated nanoclay particles. Reprinted from [10, 14] with kind permission of Elsevier
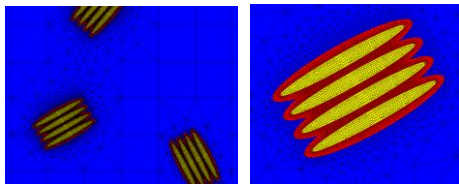

Fig. 2 – Schema of nanoparticle clustering and overlapping effective interfaces [12]

In the simulations, the transition from size-dependent nanocomposite behavior (which is observed for the particle size below 100 Å) to the size-independent microcomposite behavior was observed. While the mechanical properties of the nanocomposite improve with increasing the particle size (assuming the soft interface layer) up to the particle size 100 Å, the particle size has almost no influence on the elastic properties of the composite as soon as the particles are larger. If the effective interface layer were stiffer than the matrix, the effect would be inverse: the stiffness of the composite would decrease with increasing the particle size.

Fig. 3 shows Young modulus of composites as a function of interface overlapping (degree of nanoparticle clustering, V – real volume of effective interfaces, V_0 – volume for non-overlapping structures) and the shape of nanoparticles.

The effect of the volume fraction of nanoreinforcement on the mechanical properties of nanocomposites is determined by the interface properties. While the

stiffness of the composite increases with increasing particle volume fraction for the stiff interfaces, the effect is inverse for the soft interface.

The higher degree of particle clustering leads to lower Young's modules of the nanocomposites.
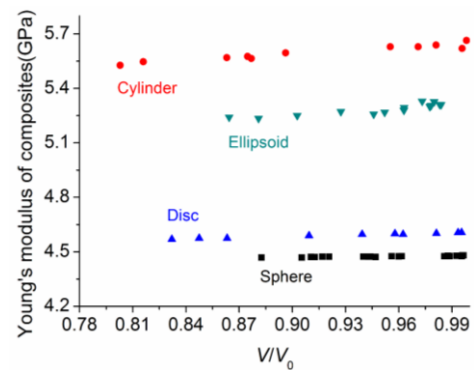

Fig. 3 – Schema of nanoparticle clustering and overlapping effective interfaces Reprinted from [12] with kind permission of Elsevier

3. DAMAGE AND FRACTURE OF NANOCOMPOSITES

In the next stage of the work, we employed 3D micromechanical modeling tools to analyze damage mechanisms and mechanics of nanoclay-reinforced polymers under mechanical loading. A 3D computational model of nanocomposites, which includes the effective interface concept and is able to account for mixed mode crack initiation and propagation, was employed.

In order to take into account different compositions and properties of the interfacial regions located between closely arranged platelets and the regions surrounding the platelets or clusters the former "three phase" model (nanoclay, effective interface and matrix) is generalized by including the "fourth phase" which is named the "intrastack interphase". In this case, the model consists of matrix, nanoplatelets, the "coating phase", surrounding single platelets in exfoliated structures or clusters in intercalated structures, respectively and the "intrastack interphase", lying between clustering nanoplatelets. As noted in [13], the intrastack phase has lower critical damage level than the usual interface.

In the simulations, different damage initiation and crack growth criteria were compared, including 3D Benzeggagh and Kenane law (BK law) criterion, the 3D Wu and Reuter law (power law) criterion and the Reeder law criterion. The effects of the platelelet aspect ratio, clustering and orientation effects on the crack propagation were studied in numerical experiments. It was observed that the increasing the aspect ratio leads to the higher Young modulus, but a lower strength of the composite. The clustering of discs has an adverse effect, meaning the increased strength and lower stiffness.

In the simulations, damage mechanisms such as crack deflection and delamination were observed. A typical damage mechanism observed in the simulations can be described as follows. A crack tends to initiate on the side of "intrastack phase" (between discs in a cluster) (not in the effective interface surrounding clusters

and single platelets). Then, the crack grows first further in the intrastack phase and then (slower) into the matrix. Delamination occurs when the crack arrives at the interface of nanoplatelet and intrastack phase, and it may lead to the crack branching. The branches can join again at the other side of delamination region or lead to two crack paths.
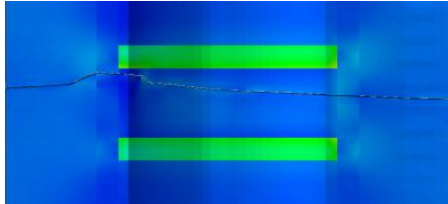

Fig. 4 – Examples of the crack propagation between two nanoplatelet in a cluster [14]
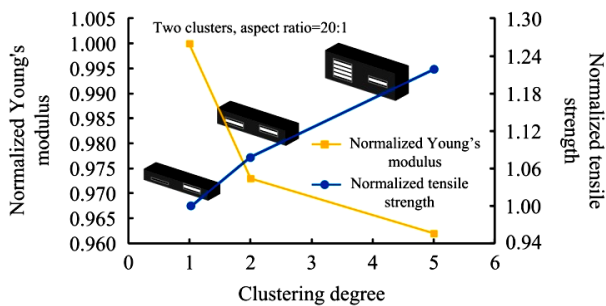

Fig. 5 – Young modulus and normalized tensile strength of nanocomposite plotted versus the clustering degree. Reprinted from [14] with kind permission of Elsevier

4. MODELLING OF HIERARCHICAL COMPOSITES

Using the estimations above, we consider the effect of nanoreinforcement on the strength of fiber reinforced composites with nanoreinforcement in the matrix.

In the simulations, we used the fiber bundle model from [15]. The volume content of fibers is 50 %. The applied stress is 1000 MPa. The weight content of nanoparticles in the matrix and the degree of intercalation z are varied. The unit cell (with one fiber) is subjected to tensile loading along the fiber direction. The probability of failure of the fiber can be calculated using the Weibull distribution function, with parameters $r_0 = 1649$ MPa and $m = 3.09$ [9]:

$$\text{Prob}\{Failure\} = 1 - \exp\left[\left(\frac{\sigma}{r_0} \frac{E_f}{E_f vc + E_{matr}(1-vc)}\right)^m\right]$$

where E_f, E_{matr} – Young's modulus of fiber, vc – volume content of fibers.

Fig. 5 shows the failure probability of fibers plotted as a function of the volume content of nanoclay in the matrix for three cases: fully exfoliated structure, and the cases with 25 % and 50 % of the intercalated particles. From the Fig. 13, it can be concluded that the failure probability of the glass fibers slightly decreases with increasing the volume content of nanoparticle in the matrix. This effect is weakened if the nanoclay particles are clustered.
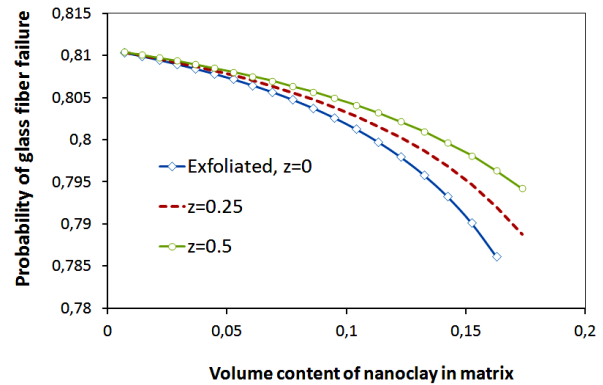

Fig. 5 – Failure probability of fibers plotted as a function of the volume content of nanoclay in the matrix for fully exfoliated structure, and cases with 25 % and 50 % of the intercalated particles. Reprinted from [15] with kind permission of Elsevier

In order to evaluate the effect of nanoreinforcement on the compressive damage, we use a unit cell model with many carbon fibers (randomly misaligned). The misalignment angles are assigned to each fiber, using random normal number generator (with truncated Gaussian probability distribution, from $-3°$ to $3°$). Then, the unit cells were subject to axial loading (or repeated loadings). For each fiber, the kinking condition is checked, according to the Budiansky-Fleck kinking condition. If one or several fibers kink, the stress is redistributed over remaining fibers, according to the power load sharing law, thus, increasing the load on remaining fibers, and the likelihood of their kinking. The following data for the unit cell model of composite were used: 100 fibers per cell, 30 % volume content of fibers, applied compressive stress 600 MPa, misalignments of fibers are randomly distributed, following the truncated Gaussian probability distribution with standard deviation 1.15°.
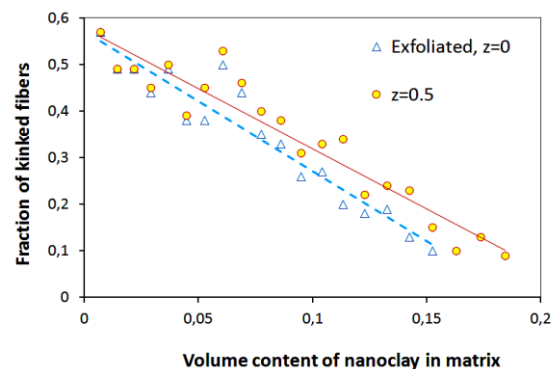

Fig. 6 – Fraction of kinked carbon fibers (compressive damage) in carbon fiber reinforced composites with nanoreinforced epoxy matrix. Reprinted from [15] with kind permission of Elsevier

Fig. 6 shows the probability of fiber kinking (fraction of kinked fibers) plotted as a function of the volume content of nanoclay in the matrix for fully exfoliated structure, and 50 % of the intercalated particles. From the Fig. 6, it can be seen that adding 10 % volume content of nanoclay to the epoxy matrix decreases the probability of fiber kinking by 72 % even for intercalated structures, and more than 2 times for

fully exfoliated structures. Thus, while the nanoreinforcement changes the probability of tensile fiber failure by just parts of a percent, it changes the probability of compressive kinking by 70…100 %.

5. CONCLUSIONS

The computational investigations presented in this work demonstrate that the nanoreinforcements and nanomodifications have a potential to improve mechanical properties, strength and stiffness of polymer fiber reinforced composites to be used for wind energy applications. The experimental studies are under way now to explore the limits of applicability of these models.

REFERENCES

1. L. Mishnaevsky Jr., P. Brøndsted, R. Nijssen, D.J. Lekou, T.P. Philippidis, *Wind Energy*, **15** No 1, 83 (2012).
2. S.U. Khan, et al., *Compos. Sci. Technol.* **70** No 14, 2077 (2010).
3. M.L. Chan, et al., *Compos. Part B: Eng.* **42**, No 6, 1708 (2011).
4. J.J. Karippal, H.N. Narasimha Murthy, K.S. Rai, M. Sreejith, M. Krishna, *J. Compos. Mater.* **22**, (2011), doi: 10.1177/002199831038908.
5. J. Xiong, Y. Liu, X. Yang, X. Wang, *Polymer Degradation and Stability* **86**, 549 (2004).
6. J.S. Shelley, P.T. Mather, K.L. DeVries, *Polymer* **42**, 5849 (2001).
7. L. Mishnaevsky Jr. *Comp. Mesomechanics of Composites* (Wiley: 2007)
8. L. Mishnaevsky Jr., P. Brøndsted *Comp. Mater. Sci.* **44**, 1351 (2009).
9. L. Mishnaevsky Jr., P. Brøndsted, *Compos. Sci. Technol.* **69**, 1036 (2009).
10. H.W. Wang, H.W. Zhou, P.D. Peng, L. Mishnaevsky Jr., *Compos. Sci. Technol.* **71**, 980 (2011).
11. H.W. Zhou, L. Mishnaevsky Jr., P. Brøndsted, J. Tan, L. Gui, *Chinese Sci. Bull.* **55** 1199 (2010).
12. R.D. Peng, H.W. Zhou, H.W. Wang, L. Mishnaevsky Jr., *Comp. Mater. Sci.* **60**, 19 (2012).
13. L. Mishnaevsky Jr., *Compos. Sci. Technol.* **72**, 1167 (2012).
14. G.M. Dai, L. Mishnaevsky Jr., *Compos. Sci. Technol.* **74**, 67 (2013).
15. L. Mishnaevsky Jr., *Compos. Sci. Technol.* **72**, 1167 (2012).